

Interactive comment on “Observationally constrained analysis of sea salt aerosol in the marine atmosphere” by Huisheng Bian et al.

Anonymous Referee #1

Received and published: 6 March 2019

Review of Observationally constrained analysis of sea salt aerosol in the marine atmosphere by Bian et al.

Reviewer: The manuscript presents valuable inter-comparison between modelled sea spray mass concentration/AOD and extensive in situ measurements. The latter is the most valuable component of this manuscript as vertical distributions of sea spray are indeed not commonly available on the large geographical scale. These measurements provide very good basis for the validation of the model, however, they were not used to their full potential in this manuscript as the appropriate sea spray source function was not provided. The main conclusion that AOD cannot be reproduced by the current model, due to wrong sea spray source function (SSSF) size distribution, is somehow disappointing without providing the appropriate one.

Answer: We thank the reviewer for the insightful comments. We have carefully accounted for the reviewer's comments and suggestions and our point-to-point response is given below.

We appreciate the reviewer's suggestion in the pursuit of establishing a new sea salt source function through our work. However, we carefully examined our currently available observation and model data and believe that the task asked by the reviewer is beyond the scope that our data can support. To achieve that goal, we need experiments that are designed specifically to measure size-resolved sea salt fluxes near air-sea interface. ATom experiment is not designed to derive a sea salt source function at a convincing precision. ATom aircraft measurement is far away from sea surface. The difference between model and measurement is not entirely attributed to sea salt emission. Any uncertainty in removal processes (e.g. wet deposition, dry deposition, and sedimentation) and dynamic transport processes contribute to the difference as well. Furthermore, the size-dependent sedimentation may reshape the sea salt size distribution away from its source regions. Based on the discrepancy between the model-calculated and ATom-observed size distributions, we can only suggest that a modification of emitted sea salt size distribution might be helpful to reduce the discrepancy.

Major comments

Reviewer: In addition to the point raised above, the appropriate comparison of the three SSSF mentioned here is not presented either; There is no discussion or results in the main text, just some numbers in the supplementary, from which it seems that Emi3 results in a higher bias than other schemes. So it is not exactly clear why it was deemed the best here? Manuscript would really benefit from more elaborate discussion on the scheme comparison as well as on how model results compare to AOD measurements using Emi1 and Emi2 schemes? Results should have short description in the main text and only then reference to supplementary (say at lines 117-119);

Answer: In the revision, we have decided to remove the supplementary material for the discussion of sea salt emission algorithms since it is not our main focus of this study.

Each experiment is designed for its specific purpose. ATom aims to provide an unprecedented suite of measurements over global remote oceans, including vertical and seasonal information of aerosol, cloud, meteorological fields. As pointed out by the reviewer, the vertical distributions of sea spray are indeed not commonly available on the large geographical scale. Combining the ATom measurements with other available satellite and ground measurements, we can evaluate our model performance on a broader scale to find out the deficiencies of the model simulation and their potential causes. In this sense, focusing on the small differences between the results using Gong 2003 and the modified ones in GEOS (as shown in the previous Supplement) would provide little help to resolve the differences.

Reviewer: Introduction section is pretty much biased on USA references, e.g. Quinn and Bates, 2013 is neither the primary nor the main study showing OM in the sea spray; also all other references are mainly from USA scientists, while there are many sea spray papers from European community that were not even mentioned here; For example, extensive SSSF overview paper by (de Leeuw et al., 2011) is missed.

Answer: We added the following reference on sea salt study by European scientists. See line 47 and references.

de Leeuw, G., Andreas, E. L., Anguelova, M. D., Fairall, C.W., Lewis, E. R., O'Dowd, C., Schulz, M., and Schwartz, S. E.: Production flux of sea spray aerosol, Rev Geophys, 49, RG2001, doi:10.1029/2010rg000349, 2011.

Reviewer: Lines 274-275: requires more information and discussion. Is this 0.03 bias comparable with the overestimation here? If not, what percentage is due to bias and what is due to other reasons;

Answer: To answer the reviewer's question, we calculated the difference of model AOD and MODIS AOD over oceans where the fraction of sea salt AOD is higher than 0.6. Overall, MODIS AOD is larger than model AOD by 0.043 in August 2016 and 0.062 in February 2017. Both differences are larger than the potential positive bias of MODIS AOD, up to 0.03, over oceans. However, it is hard for us to figure out the percentage contributions asked by the reviewer. The reason is that the work of Levy et al. (2013) gave only statistic value of MODIS AOD bias without the information of geophysical location. We added the new calculation and corresponding discussion in section 4.3 lines 284-290.

Reviewer: Lines 302-304: I understand that the reference is to mass size distribution here, but radiative effects and cloud formation depend more on the number distribution, not mass.

Be clear which distribution you refer to and be specific with the effects; Or Lines 313-314, cloud formation is related to size and number not mass;

Answer: We agree with the reviewer that radiative effects and cloud formation depend on the number of aerosol particles. This is why we studied the sea salt size distribution and emphasized the importance of the sea salt aerosols in the fine mode size in the paper. In lines 314-315, we changed the sentence to "Aerosol size also modulates the transport and removal processes. In lines 324-328, we emphasized the role of sea salt number particles by changing the sentence to "The particle sizes here are limited to be less than 3 μm in dry diameter due to the size cut of the PALMS inlet. Particles in this range are most important in light extinction and cloud formation with many more sea salt particles in fine mode than in coarse mode on a per unit mass basis."

Reviewer: Conclusion on sea water salinity is not convincing globally (lines 400-403), what is salinity variation in global oceans? It might be important locally or regionally close to less saline seas, but not globally;

Answer: Yes. Salinity may not be an important factor in sea salt emission on the global scale because it is relatively uniform across the world oceans. But regionally it may be important as discussed by Grythe et al., (2014). Our model does not account for the salinity impact at all so that the model sea salt results may be low over cold low saline seas, such as the Baltic Sea. We changed the sentences on lines 419-425 in Conclusion to the following. “Consideration of variations in salinity of surface seawater is missing in the GEOS aerosol model. Although salinity may not be an important factor in sea salt emission on the global scale owing to its relatively uniformity across the world oceans, it may be important regionally as discussed by Grythe et al., (2014). Salinity also impacts sea spray aerosol (SSA) size. The dry SSA size distribution shifts towards smaller sizes with lower salinities found in the EMEP intensive campaigns (Barthel et al., 2014).”

Reviewer: Similarly with the Polar Regions (lines 403-407), indicate how sea ice is relevant to this global study? Is there a higher discrepancy over Polar Regions, if so state that and show the importance?

Answer: The study of potential sea salt from sea ice is not directly relevant to the main study of this work. Similar to the discussion for salinity, here we tried to give any other potential improvements on global sea salt simulation based on recent scientific publications and our knowledge.

Reviewer: Elaborate on the conclusion sentence in supplementary ‘Furthermore, the three emission algorithms discussed in supplementary section show that the uncertainty among the model simulations is generally less than the difference between model and measurement’. First, algorithms do not show anything, comparison, maybe, second, does this sentence mean that the discrepancy between model and measurements is larger than the model result variation between different SSSF? Clarify. Authors claim that ‘ Model sensitivity experiments indicated that the simulated sea salt is better correlated with measurements when the sea salt emission is calculated based on the friction velocity and with consideration of sea surface temperature dependence than that parameterized with the 10-m winds’ but these results are not properly discussed or presented in the text. Supplementary figures and tables also do not clearly prove that Emi3 is better than other schemes. Correlation might have improved, but the bias got worse. Can you base the conclusion on correlation only?

Answer: The supplementary material has been removed with the reasons aforementioned.

Specific comments:

Reviewer: Line 161: provide the correlation coefficient;

Answer: Line 161: The correlation coefficient between the two instrument measurements was given in section 4.1 lines 220-221.

Reviewer: Line 57-58: Dall et al., 2017 reference is not in the list; Quinn et al., 2017 paper says that sea spray is not important for cloud formation, so the reference is not appropriate here

Answer: Dall et al., 2017 was listed in the reference. We removed Quinn et al., 2017 and added one more recent relevant study of Dall et al., 2018.

Reviewer: Fig. 2: add ‘3’ to superscript in both axis names; Do three significant number have meaning in the correlation coefficient and slopes (are they really so precise?);

Answer: Done. We guess the question here is about the steps we applied for measurement data quality control. Yes, these are necessary steps for our data analyses. Otherwise, the interpreted sea salt measurement will be contaminated by dust- Na^+ and clouds. For example, the difference in correlation coefficient and ratio between Figure 2a and 2b is caused by cloud droplets or ice crystals acting like a high-pressure washer to dislodge some of that salt in forward-facing aircraft inlet.

Reviewer: Fig.2 and lines 188-189: R square is usually presented for model-measurement comparisons, have either R^2 or both Lines

Answer: Using R or R^2 depends on what kind of comparison we investigate. Here we use R to give a point-to-point correlation between the model and measurement data. By the reviewer's suggestion, we added in the text of R^2 to estimate the covariance of the two datasets, see lines 199-200.

Reviewer: 245-246: 90% in the mass, not number, provide reference;

Answer: The sentence (lines 256-257) has been changed to "This is expected because nearly 90% of injected sea salt mass is in coarse mode based on our emission scheme."

Reviewer: Lines 281-283: sentence needs rewriting, simulation occurred in July or measurements over this period were compared? Conclusion cannot be obtained in Fig.5. Fig 5 indicates: : :?

Answer: The sentence (lines 296-298) has been changed to "MAN measurements from July, 2016 to June 2017 are used in this study. The GEOS model results are sampled at the closest time and location of the ship-based measurements." Figure 5 does show GEOS AOD is significantly lower than MAN AOD over sea salt dominant regions.

Reviewer: Lines 300-301: specify what do you mean by 'small particles are more optically efficient' do they scatter better or worse? It is commonly accepted that large particles scatter better; Also, refer to size ranges when talking about small or large particles (here and everywhere in the manuscript) ; E.G line 312: what is small here;

Answer: It is true that generally the larger a particle is, the more scattering it has. However, traditional aerosol models simulate aerosol masses. Obviously, on a unit mass basis, fine mode sea salt has a larger cross section than that of coarse mode sea salt. To clarify the fine mode sea salt discussed in the paper, a sentence was added in section 2 lines 140-141: "We further classify the first two bins as fine mode and the remaining bins as coarse mode throughout this paper."

Reviewer: Line 318: efficiency?

Answer: Yes. Changed the word to be "efficiency".

Reviewer: Line 370: with which SSSF the agreement between model and measurements is remarkable?

Answer; The discussion was based on our default sea salt emission algorithm. Also refer to the answer on the last two questions of reviewer #2.

Reviewer: Line 406: Dall et al. 2017 reference is not in the reference list;

Answer: See the answer on the question for "line 57-58" above.

Reviewer: Table 1: Emi1, Emi2, : : are not described in the text or table caption;

Answer: We removed Emi1 and Emi2 according to our discussion above. We also merged Table 1a and 1b to Table 1 and changed text accordingly.

Reviewer: Supplementary Line 40: Emi3 is improved for total mass not size distribution. Supplementary Lines 70-71: what do you mean by shifts? Supplementary Line 75: higher than what? Supplementary Line 82: improvement from 0.5 to 0.54 might be perceived as marginal, no?

Answer: Supplementary material has been removed.

Reviewer: Why there is such big difference in Atom1 and Atom2 agreements, correlations?

Answer: This is not an easy question to answer. Size cut changes and a correction factor may both contribute. Say, if ATom2 MBL was slightly wetter on average than ATom1 then PALMS dry SS size cut would be slightly lower and produce this result. The PALMS team had to apply a correction to the size distribution data in ATom2 (described in Murphy et al., 2019) to make it more consistent with the SAGA measurement. Of course, GEOS sea salt may also have a seasonal bias. We need additional independent measurements to evaluate this issue.

Anonymous Referee #2

Received and published: 24 March 2019

General comment:

Reviewer: This manuscript examines the vertical profile of sea salt aerosol concentrations obtained during the NASA Atom campaign, and evaluate the model's capability in reproducing the observations. The Atom observations offer unique vertical distributions of sea salt aerosols over the ocean, and thus provide some critical insight on the source function of sea salt aerosols. In this work, they chose a source function based on the surface friction velocity and sea surface temperature, and found that the model overestimates the observed sea salt aerosol mass concentrations, but underestimates the AOD over the sea salt dominated area. They suggest that it can be due to the discrepancy in modeled size distribution or relative humidity, pointing the necessity for further investigation to improve the sea salt parameterization. Overall, this work provides insightful information on improving parameterization of sea salt aerosols, and I support the publication of this work in ACP if they can address the following specific comments.

Answer: We thank the reviewer for the insightful comments. We have carefully accounted for the reviewer's comments and suggestions and our point-to-point response is given below.

Specific comment:

Reviewer: Line 114: How well is the surface friction velocity being represented in the model? For example, what is the range of error when compared to observations?

Answer: The ocean surface wind of GEOS Modern-Era Retrospective Analysis for Research and Applications version 2 (MERRA2) is directly assimilated using two satellite observations, Special Sensor Microwave Imager (SSM/I) and Quick Scatterometer (QuikSCAT) (Rienecker et al., 2011, appendix B). We run the GEOS model using "replay mode", which means every 6h the model dynamic state including these surface winds is set to the state of MERRA2. We added a sentence in lines 122-124. "The model's surface winds are constrained by the two satellite observations, Special Sensor Microwave Imager (SSM/I) and Quick Scatterometer (QuikSCAT) (Rienecker et al., 2011)."

Reviewer: Line 161: How is the cut-off diameter of SAGA measurement? How does that compared to PALMS? Figure 2ab shows that the modeled SS seems to be underestimated when compared to the SAGA data, and overestimated while compared to the PALMS? Is it potentially due to the different cut-off diameter? What are the measurement uncertainties of SS in PALMS and SAGA?

Answer: The cut-off diameter of SAGA measurement is roughly the same as PALMS's under the marine boundary environment according to the study of the DC-8 Inlet Characterization Experiment (DICE) (McNaughton et al., 2007). We added this sentence in lines 177-178: "In other words, the cut-off size of the SAGA instrument is also roughly 3 μ m in dry diameter." According to the instrument PIs, the uncertainty is not straightforward, but the precision uncertainty of PALMS in SS mass in the MBL is ~10% and overall uncertainty is probably about ~30% (Froyd et al., 2019). The precision uncertainty of SAGA is ~30% as well. Please also see our discussion for the instrument uncertainties in lines 210-216.

Froyd, K. D., Murphy, D. M., Brock, C. A., Campuzano-Jost, P., Dibb, J. E., Jimenez, J.-L., Kupc, A., Middlebrook, A. M., Schill, G. P., Thornhill, K. L., Williamson, C. J., Wilson, J. C., and Ziemba, L. D.: A new method to quantify mineral dust and other aerosol species from aircraft platforms using single particle mass spectrometry, Atmos. Meas. Tech. Discuss., <https://doi.org/10.5194/amt-2019-165>, in review, 2019.

Reviewer: Line 211: Although the sea salt between two instruments shows high correlations, is it possible that one of the measurements is consistently higher than the other one?

Answer: Yes, it is. The SAGA sea salt mass is consistently higher than the PALMS sea salt.

Reviewer: Line229: What is the vertical resolution of PALMS, and how does that compared to GEOS5? It seems that the model had a hard time catching some of the features in the higher troposphere.

Answer: The vertical profile of PALMS is based on 3-min averages, which gives a vertical resolution of 2.3 km. Statistical noise becomes large at low mass concentrations of ~1-10 ng/m³ and will contribute to the structure in PALMS SS mass in the upper troposphere. In the meanwhile, the vertical resolution of GEOS could reach ~1 km in the upper troposphere. The missing features there in the model data could also be attributed to the model's vertical and long-range transport.

Reviewer: Line 269: Just curious, what is the most abundant aerosol over the Arctic Ocean, as sea salt only contribute to 10-50% as shown in Figure 4 bottom?

Answer: The most abundant aerosols over the Arctic Ocean are sea salt (10-50%), sulfate (up to 40%), dust (up to 30%) and organic carbon (up to 20%) based on the GEOS results.

Reviewer: Line 270: What is the cut-off diameter for the sea salt aerosols in the modeled AOD?

Answer: The cut-off diameter for the sea salt aerosols in the modeled AOD is 20 μ m. Please refer to the model description in section 2 lines 136-137 for details.

Reviewer: Line 276: Is the underestimate of AOD consistent around the globe? Or certain latitudes/SSTs have relatively smaller underestimates?

Answer: No. The AOD underestimation occurred primarily over ocean regions. In land anthropogenic and dusty pollution areas, the model sometimes overestimates AOD. We did the model and ATom comparison over five latitudinal bands, as shown in Figure 3, and we did not find an obvious latitudinal dependence in the model performance.

Reviewer: Which factor(s) do you think is/are most critical for improving the sea salt parameterization?

Answer: Improvement of sea salt size distribution, particularly the ultrafine particles, is suggested based on our study. Current GEOS model sea salt emission parametrization generally gives a low-bound cut-off diameter at around 100 nm in dry diameter. This seems not sufficient, and we suggest to extend it down to 10 nm. Particles smaller than 80 nm in diameter can effectively become CCN through heterogeneous growth and coagulation with other sub-80 nm particles [Clarke et al., 2006], although generally a minimum dry diameter of 80 nm is considered for cloud activation [Pierce et al., 2006].

Clarke, A. D., Owens, S. R. & Zhou, J. 2006 An ultrafine sea-salt flux from breaking waves: implications for cloud condensation nuclei in the remote marine atmosphere. J. Geophys. Res. 111, D06202. (doi:10.1029/2005JD006565)

Pierce, J. R. and Adams, P. J.: Global evaluation of CCN formation by direct emission of sea salt and growth of ultrafine sea salt, J. Geophys. Res., 111, D06203, doi:10.1029/2005JD006186, 2006.

Reviewer: What measurement would you suggest to improve the sea salt parameterization?

Answer: To improve the sea salt parameterization, we need to put more effort on the measurements of size-resolved sea salt flux at various ocean surfaces, such as oceans with different latitudes, seasons, winds, temperatures, salinities, and marine ecosystems. We need to pay particular attention to ultrafine sea salt.

Reviewer: Table 1ab: Please write out the words or explain in the captions the abbreviation (such as SV deposition).

Answer: Done.

Reviewer: Figure 1ab: Please explain in the figure captions that what is r(correlation?) and b (bias?).

Answer: Done for Figure 2ab. Here, the statistical parameter r is the correlation coefficient and b is the ratio of $SS(GEOS)$ to $SS(ATom)$.

Reviewer: Figure 3. Please provide the vertical metric in height (km or m) if possible.

Answer: Done.

Reviewer: Figure 4. Please explain what is fss in the caption.

Answer: Done. We changed fSS to $fSSAOD$, which is the fraction of sea salt AOD versus total aerosol AOD.

Comment for Supplement

Reviewer: Line 55: Could you please provides some details on how 2.41 is derived here (or the related reference)?

Answer: The functional form of the wind- and SST-dependent terms were developed and used in the MERRA2 meteorology and aerosol reanalysis (Darmenov et al, 2013; Randles et al., 2013). Examination of the wind term based on Gong's parameterization was prompted by the presence of high/low bias in sea

salt aerosol optical depth (AOD) in high/low latitudes in the GEOS model. To address this bias we analyzed the relationship between sea salt AOD and friction velocity, and concluded that the power factor of 3.41 is too high and should be lowered by about unity (or 2.41). With that change the sea salt emissions and sea salt AOD in GEOS became more uniform and with less pronounced zonal gradient. We would like to point out that the power factor of 2.41 is well within the range of values reported by other studies (see for example compilation of 10-meter wind and friction velocity parameterizations by Anguelova et al. (2006) and more recently by Brumer et al. (2017)). Similarly to Jaegle et al. (2011), we examined the remaining differences between the model and satellite AODs (when sea salt had significant contribution to the total AOD), and attributed these to the effects of SST on sea salt emissions by parameterizing the ratio of observed to modeled AOD as a function of SST. The SST used at the time in GEOS was from the Reynolds dataset.

This work is not attempting to develop or modify the GEOS sea salt emission. Rather we intend to suggest a direction in improving emitted sea salt size distribution that might be helpful to reduce the discrepancy between the model-calculated and ATom-observed size distributions. Please also refer to our answers to the major comment of reviewer #1

Anguelova, M. D., and F. Webster (2006), Whitecap coverage from satellite measurements: A first step toward modeling the variability of oceanic whitecaps, J. Geophys. Res., 111, C03017, doi:10.1029/2005JC003158.

Brumer, S.E., C.J. Zappa, I.M. Brooks, H. Tamura, S.M. Brown, B.W. Blomquist, C.W. Fairall, and A. Cifuentes-Lorenzen, 2017: Whitecap Coverage Dependence on Wind and Wave Statistics as Observed during SO GasEx and HiWinGS. J. Phys. Oceanogr., 47, 2211–2235, <https://doi.org/10.1175/JPO-D-17-0005.1>

Darmenov, A., da Silva, A., Liu, X. and Colarco, P. R., (2013), Data-driven aerosol development in the GEOS-5 modeling and data assimilation system, Abstract A43D-0305 presented at 2013 Fall Meeting, AGU, San Francisco, Calif., 9-13 Dec.

Jaeglé, L., Quinn, P. K., Bates, T. S., Alexander, B., and Lin, J.-T.: Global distribution of sea salt aerosols: new constraints from in situ and remote sensing observations, Atmos. Chem. Phys., 11, 3137–3157, <https://doi.org/10.5194/acp-11-3137-2011>, 2011

Randles, C.A., A.M. da Silva, V. Buchard, P.R. Colarco, A. Darmenov, R. Govindaraju, A. Smirnov, B. Holben, R. Ferrare, J. Hair, Y. Shinozuka, and C.J. Flynn, 2017: The MERRA-2 Aerosol Reanalysis, 1980 Onward. Part I: System Description and Data Assimilation Evaluation. J. Climate, 30, 6823–6850, <https://doi.org/10.1175/JCLI-D-16-0609.1>

Reviewer: Line 65: Do you mean the correction factor, $T(SST)$, ranges from 0.0 to 7 here? I tried to calculate it, and it shows that at 36degreeC, the correction factor is 10.63. Also, at -0.1 degree C, it is 0.36? Is this due to rounding? Please double check. Also, please provide a plot of $T(SST)$ versus SST, if possible. And please provide details on how these correction factors are derived (or the related reference).

Answer: Your calculation is right. The $T(SST)$ will start from 0.4 when SST is close to frozen point. Since $T(SST)$ is confined to be less than 7, the corresponding up-bound SST should be around 34.6. In our model calculation, we run SST from 0 up to 36.0 and reset $T(SST)$ to be 7 when it is larger than 7. The figure of $T(SST)$ versus SST is provided here. Please refer the answer to “Line 55” for the derivation of temperature correction.

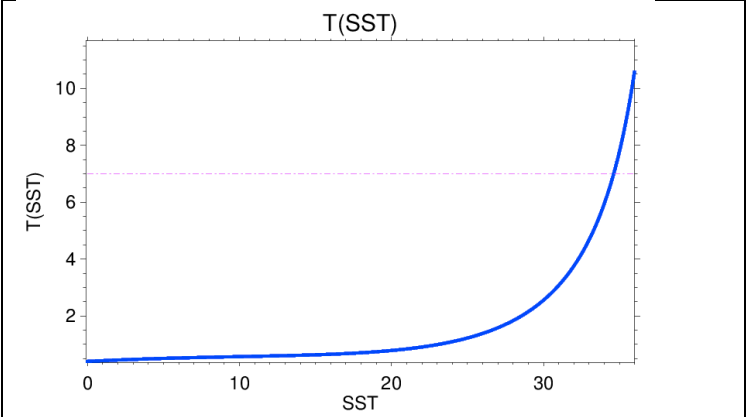


Figure shows the relationship between T(SST) and SST.

1 **Observationally constrained analysis of sea salt aerosol in the**
2 **marine atmosphere**

3

4 Huisheng Bian^{1,2}, Karl Froyd^{3,4}, Daniel M. Murphy³, Jack Dibb⁵, Anton Darnenov², Mian Chin²,
5 Peter R. Colarco², Arlindo da Silva², Tom L. Kucsera⁶, Gregory Schill^{3,4}, Hongbin Yu², Paul Bui⁷,
6 Maximilian Dollner⁸, Bernadett Weinzierl⁸, and Alexander Smirnov⁹

7 ¹ University of Maryland at Baltimore County, Baltimore County, MD

8 ² NASA Goddard Space Flight Center, Greenbelt, MD

9 ³ NOAA Earth System Research Laboratory, Chemical Sciences Division, CO

10 ⁴ Cooperative Institute for Research in Environmental Sciences, University of Colorado, Boulder, CO

11 ⁵ University of New Hampshire, Durham, NH

12 ⁶ Universities Space Research Association, Columbia, MD

13 ⁷ NASA Ames Research Center, Moffett Field, CA

14

15 ⁸ University of Vienna, Faculty of Physics, Aerosol and Environmental Physics, Boltzmannngasse 5, A-
16 1090 Wien, Austria

17

18 ⁹ Science Systems and Applications, Inc., Lanham, MD 20706

19

20 **Abstract**

21 Atmospheric sea salt plays important roles in marine cloud formation and atmospheric
22 chemistry. We performed an integrated analysis of NASA GEOS model simulations run
23 with the GOCART aerosol module, *in situ* measurements from the PALMS and SAGA
24 instruments obtained during the NASA ATom campaign, and aerosol optical depth
25 (AOD) measurements from AERONET Marine Aerosol Network (MAN) and from
26 MODIS satellite observations to better constrain sea salt in the marine atmosphere.
27 ATom measurements and GEOS model simulations both show that sea salt

28 concentrations over the Pacific and Atlantic oceans have a strong vertical gradient,
29 varying up to four orders of magnitude from the marine boundary layer to free
30 troposphere. The modeled residence times suggest that the lifetime of sea salt particles
31 with dry diameter less than 3 μm is largely controlled by wet removal, followed next by
32 turbulent process. During both boreal summer and winter, the GEOS simulated sea salt
33 mass mixing ratios agree with SAGA measurements in the marine boundary layer (MBL)
34 and with PALMS measurements above the MBL. However, comparison of AOD from
35 GEOS with AERONET/MAN and MODIS aerosol retrievals indicated that the model
36 underestimated AOD over the oceans where sea salt dominates. The apparent discrepancy
37 of slightly overpredicted concentration and large underpredicted AOD could not be
38 explained by biases in the model RH affecting the particle hygroscopic growth as
39 modeled RH was found to be comparable to or larger than the *in_situ* measurements. This
40 conundrum could at least partially be explained by the difference in sea salt size
41 distribution; the GEOS simulation has much less sea salt percentage-wise in the smaller
42 particle size range, thus less efficient light extinction, than what was observed by
43 PALMS.

44

45 **Introduction**

46 Bubble bursting and jet drops at the ocean surface result in the production of sea spray
47 particles composed of inorganic sea salt and organic matter (e.g., [de Leeuw et al., 2011](#);
48 Quinn and Bates, 2013). Among various atmospheric aerosol components, sea salt is
49 estimated to have the largest mass emission flux and the second largest atmospheric mass
50 loading globally (Textor et al., 2006). Sea salt particles in the atmosphere could exert

51 direct radiative effect of around -1.5 to -5.03 W/m² annually at the top of atmosphere
52 (IPCC, 2001). On a global and annual scale, the direct radiative effect of sea salt is equal
53 to or greater in magnitude than that of natural sulfate and soil dust (Jacobson, 2001;
54 Takemura et al., 2002). Sea salt particles are efficient cloud condensation nuclei (CCN).
55 Consequently, sea salt particles have indirect effects on climate and weather
56 (Dadashzaer et al., 2017; Dall et al., 2017, 2018; Kogan et al., 2012; Pierce and Adams,
57 2006). Furthermore, sea salt aerosol particles serve as sinks for reactive gases and small
58 particles and are a source of halogens to the atmosphere (e.g., Alexander al., 2005;
59 Anastasio et al., 2007; Lawlet et al., 2011). There is also observational evidence
60 suggesting that new particle formation may be suppressed in the presence of sea salt
61 aerosol (Browse et al., 2014; Lewis and Schwartz, 2004). To quantify the effects of sea
62 salt aerosol on the environment, a detailed knowledge of its mass, size, and vertical
63 distribution is required. However, measurements of sea salt are not only sparse but also
64 mostly limited to near the surface at a few locations (Prospero et al., 2003), posing
65 difficulties in assessing the global environmental effects of sea salt as well as evaluating
66 model skill at simulating sea salt vertical distributions and properties.
67
68
69 A recent NASA-funded Earth Venture-suborbital project, the Atmospheric Tomography
70 Mission (ATom), deployed an extensive gas and aerosol instrumental payload on the
71 NASA DC-8 aircraft for systematic, global-scale sampling of the atmosphere in four
72 seasons over a 3-year period (2016-2018), profiling continuously from 0.2 to 12 km
73 altitude with flight routes over the Pacific, Atlantic, Southern Ocean, North America and

74 Greenland from 85°N to 65°S (see Fig. 1). For the first time, vertical profiles of sea salt
75 aerosol concentration and size distribution are measured in ATom over vast oceanic
76 routes in different seasons, providing an unprecedented opportunity for models to
77 evaluate transport and parameterizations of physical and chemical processes.

78

79 We present in this study a comprehensive evaluation of sea salt aerosol simulated with
80 the Goddard Chemistry, Aerosol, Radiation, and Transport model (GOCART) in the
81 Goddard Earth Observing System (GEOS) framework using aerosol measurements
82 obtained during the first two ATom deployments, which represent the summer and winter
83 seasons for both hemispheres. We utilize ATom's high frequency vertical measurements
84 of sea salt over global remote oceans from the marine boundary layer (MBL) to the upper
85 troposphere, in contrast with previous model validations of sea salt simulation performed
86 with *in situ* measurements at the surface and over limited selected locations and regions
87 (Chin et al., 2014; Kishcha et al., 2011; Spada et al., 2013, 2015; Tsyro et al., 2011;
88 Witek et al., 2007) and typically using only monthly averaged observations (Grini et al.,
89 2002; Textor et al., 2006). We compare the model simulated sea salt vertical
90 distributions with observations in various latitudinal zones over the Pacific and Atlantic
91 oceans, refer to dry and wet deposition processes, and examine the sea salt size
92 distribution that is important to both AOD calculations and cloud formation.

93

94 The GEOS/GOCART model is described in section 2, particularly the sea salt emission
95 scheme used in this study. The NASA ATom field campaign is introduced in section 3,
96 including a brief description of the Particle Analysis by Laser Mass Spectrometry

97 (PALMS) and Soluble Acidic Gases and Aerosols (SAGA) instruments that are used to
98 provide sea salt measurements. [Measured and modeled vertical profiles, size](#)
99 [distributions, and AOD are compared to assess model emissions and removal processes](#)
100 [in section 4](#). In section 5, we summarize [the outcome of](#) our study and discuss the
101 potentially important chemical/physical processes that [likely](#) have an impact on sea salt
102 simulation [and recommend](#) future improvements.

103

104 **Model description**

105 Global [aerosol](#) is simulated by GEOS/GOCART, which is a global aerosol model
106 GOCART (Chin et al., 2002, 2014) implemented in the GEOS Earth system model
107 (Gelaro et al., 2017; Rienecker et al., 2011). The GEOS/GOCART aerosols include dust,
108 sea salt, sulfate, nitrate, ammonium, black carbon, and organic matter, mixed externally
109 (Bian et al., 2013; 2017; Colarco et al., 2010).

110

111 [Sea salt emissions are controlled by aerosol particles generated from collapsing bubbles](#)
112 [and ejected jet droplets that in turn are directly related to the whitecap fraction in the](#)
113 [ocean and are commonly parameterized as a function of wind speed and SST](#). The sea
114 salt emission scheme in the GEOS/GOCART model was initially based on the algorithm
115 of Gong (2003) who provided a parameterization of the size-resolved flux of sea salt
116 particles as a function of the 10-m wind speed. Two modifications to this scheme were
117 subsequently developed based on comparisons of simulated sea salt aerosol to satellite
118 AOD from the Moderate Resolution Imaging Spectroradiometer (MODIS) (Darmenov et
119 al., 2013; Randles et al., 2017): 1) the emission function was recalibrated in terms of the

120 surface friction velocity rather than the 10-m wind speed and 2) a sea surface temperature
121 (SST) correction term [that is similar to the work of Jaeglé et al. \(2011\)](#) was introduced.
122 The model's surface [winds are](#) constrained by the two satellite observations, Special
123 Sensor Microwave Imager (SSM/I) and Quick Scatterometer (QuikSCAT) (Rienecker et
124 al., 2011). [This](#) emission algorithm is the default GEOS/GOCART sea salt emission and
125 is used in this study.

126
127 The current default setting of GEOS/GOCART allows sea salt to be completely removed
128 by warm clouds from convective updraft and from large-scale rainout and washout. Sea
129 salt can also be removed by dry deposition (turbulent) and sedimentation. These
130 processes were described in Chin et al. (2002). We assume that the particles undergo
131 hygroscopic growth according to the equilibrium parameterization of Gerber (1985),
132 which is a function of the relative humidity (RH). The humidified particle sizes are
133 considered in our computations of the particle sedimentation, aerodynamic deposition
134 velocity, and optical properties.

135
136 The GEOS/GOCART includes five bulk sea salt size bins in the range of 0.06-20 μm in
137 dry diameter. Specifically, they are 0.06-0.2, 0.2-1.0, 1.0-3.0, 3.0-10, and 10-20 μm ,
138 respectively. The first bin was [not included in the previous GOCART versions \(Chin et](#)
139 [al., 2002, 2014\)](#), but was added to facilitate aerosol-cloud [interactions](#) and optical
140 property studies (Colarco et al. 2010). We further [classify](#) the first two bins as fine mode
141 [and the remaining bins as coarse mode throughout this paper](#). The sea salt particle density
142 is 2200 (kg/m^3) for all sizes.

143

144 In this study, we ran GEOS/GOCART at a global ~50 km horizontal resolution on the
145 cubed-sphere grid and 72 vertical layers from surface to 0.01 hPa. We ran the model in
146 the “replay” mode, which sets the model dynamical state (winds, pressure, and
147 temperature) at every 6 hours to the balanced state provided by the meteorological
148 reanalysis fields from the Modern-Era Reanalysis for Research and Applications version
149 2 (MERRA-2). An 18 month simulation was conducted from the beginning of 2016 to
150 cover the first two phases of ATom measurement periods, with the first half year as a
151 spin up period.

152

153 **ATom aircraft sea salt measurement from PALMS and SAGA**

154 ATom provides measurements for various important atmospheric gases, aerosols and
155 their precursors over vast open oceans. Among these, sea salt has been measured by two
156 instruments, the NOAA PALMS instrument, which provides mass mixing ratio and size
157 distribution up to 3 μm in dry diameter, and the University of New Hampshire SAGA
158 instrument, which includes measurements of sodium ion (Na⁺) as a proxy of sea salt.

159 PALMS is a laser ionization mass spectrometer which makes *in situ* measurements of the
160 chemical composition of individual aerosol particles. A detailed description of PALMS,
161 including its physical working mechanism and measurement features, has been given by
162 Murphy et al., (2019) and Froyd et al., (2019). The instrument is capable of measuring
163 particles from 0.12 to 3 μm in dry diameter and analysis is completed in less than 1
164 millisecond after the aerosols enter the inlet. The real power of the PALMS sea salt
165 measurements is twofold: a) high sensitivity at low concentrations above the MBL such

166 that the measured vertical profiles are more reliable than most previous data, and b) the
167 data are size-segregated up to 3 μm in dry diameter, covering the active size range for
168 optical and radiative calculations.

169 On the other hand, the sea salt aerosol mass concentration from SAGA is deduced by
170 applying a factor of 3.27 to the measured Na^+ mass concentration (Keene et al., 1986;
171 Wilson, 1975). This assumes that all of the measured Na^+ comes from sea salt, which
172 should be a reasonable assumption for most ATom samples. SAGA collects particles on a
173 filter with a sampling frequency of around 5-15 minutes to allow more time for the filter
174 media to collect sufficient particles. As reported by the DC-8 Inlet Characterization
175 Experiment (DICE), the SAGA inlet performed nearly identically in the marine boundary
176 environment to the U. Hawaii inlet used by PALMS during ATom (McNaughton et al.,
177 2007). In other words, the cut-off size of the SAGA instrument is also roughly 3 μm in
178 dry diameter. As shown in Murphy et al. (2019), sea salt concentrations inferred from the
179 SAGA sodium data are highly correlated with PALMS sea salt data in the cloud-free
180 MBL.

181
182 We use ATom1 (Jul.-Aug., 2016) and ATom2 (Jan.-Feb., 2017) campaign data in this
183 study. These two deployments combined together provided detailed information for
184 summer and winter on a global scale.

185

186 **Results and Discussions**

187

188 **4.1 Comparisons in the marine boundary layer**

189 Sea salt is sufficiently rich in the MBL that SAGA can collect enough aerosol there for
190 analysis. Comparisons of the sea salt in a layer from surface up to 1.5 km between the
191 model simulation and ATom (PALMS and SAGA) measurements are shown in Fig. 2a.

192 To have a proper comparison, we made three data treatments. First, we excluded SAGA
193 samples with significant dust signal, identified when the measurements meet the two
194 conditions: Ca^{2+} greater than $0.05 \mu\text{g}/\text{sm}^3$ and the ratio of Ca^{2+} to Na^+ greater than 0.06.
195 Second, we only include GEOS sea salt particles smaller than $3 \mu\text{m}$ in dry diameter in
196 order to be consistent with the instrument measurements. Third, we sampled GEOS and
197 PALMS data at the SAGA measurement time frequency when the SAGA has valid
198 measurements. The correlation coefficients (R) between the model and PALMS or
199 SAGA data are generally higher than 0.79 and the covariance (R^2) higher than 0.64 in
200 both ATom1 and 2 periods.

201

202 There are outliers on the Figure 2a. Just a small amount of cloud can wash off salt
203 previously deposited on an inlet wall. Therefore, in Figure 2b we excluded samples that
204 might be contaminated by clouds during sampling, using a cloud indicator from the
205 Cloud, Aerosol, and Precipitation Spectrometer (CAPS). The outliers are gone on Figure
206 2b and the correlation coefficients between model and measurements are indeed
207 improved from 0.82-0.84 to 0.85-0.87. On the other hand, the GEOS sea salt mass mixing
208 ratios are still more than double of those of PALMS (2.3 in ATom1 and 4.7 in ATom2),
209 which could be at least partially explained by potential sampling biases in PALMS
210 instrument, particularly in the size distribution. The cut-off at $3 \mu\text{m}$ in dry diameter is
211 recommended by the instrument teams, it is known that this is subject to a large

212 uncertainty of wet/dry size ratio that is strongly dependent on ambient relative humidity.
213 Furthermore, the sea salt mass distribution is (sometimes) still rising sharply through the
214 inlet cutpoints. Considering the combination of all these systematic and random
215 uncertainties, which are decreased across the sea salt coarse mode, the measurement can
216 easily result in uncertainties on the order of ~2x in dry mass. When checking the
217 comparison between GEOS and SAGA, GEOS sea salt mixing ratio is comparable to or
218 slightly larger than SAGA results (i.e. [ratio of GEOS to SAGA is](#) 0.92 in ATom1 and 1.3
219 in ATom2). Overall, the GEOS is most likely to overestimate sea salt mass [during](#)
220 [February](#). Comparing sea salt between the two instruments directly shows a high
221 correlation (0.81 in ATom1 and 0.94 in ATom2) as well (also see Murphy et al., 2019).

222

223 **4.2 Vertical distribution**

224 Understanding the sea salt vertical distribution is important, particularly in the tropical
225 marine upper troposphere where a reliable background aerosol field is needed. However,
226 most previous sea salt measurements were limited to the surface or near coastal areas,
227 leading to nearly no *in situ* observations of the vertical distribution of sea salt over vast
228 areas of the open oceans. The ATom measurements fill this gap by providing
229 measurements over the Pacific, Atlantic, and Southern oceans from near surface to the
230 upper troposphere (0.2-12 km). Furthermore, the PALMS instrument measures *in situ* sea
231 salt mass and size distribution. [The high](#) sensitivity of the PALMS [instrument](#) makes its
232 [data](#) very useful in studying the relatively clean environments above the MBL. Using the
233 ATom sea salt measurements over remote open oceans has some additional advantages
234 [over](#) previous studies. For instance, airborne measurements alleviate biases typical at land

235 stations due to onshore wave breaking activities, especially at sites with steep topography
236 (Witek et al., 2007; Spada et al., 2015).

237

238 Figure 3 shows the sea salt vertical profiles of PALMS measurement and GEOS model
239 simulation over 5 latitudinal zones over Pacific and Atlantic oceans in ATom1 and
240 ATom2. The GEOS model results are sampled at the time and location closest to the
241 measurement points. As discussed in section 4.1, modeled sea salt mass concentrations
242 are higher than the PALMS data near the surface over all latitudinal zones during both
243 summer and winter seasons.

244

245 There are often two vertical regimes: a sharp gradient of sea salt in the lower atmosphere
246 and a lesser gradient above. Wet removal processes, particularly convective cloud
247 removal, are likely the driving factors for the sea salt distribution in the size range
248 considered in this study (Table 1 column 2). Sea salt is a highly soluble species. It is
249 assumed to fully dissolve in clouds, resulting in efficient removal by shallow marine
250 clouds, typically marine stratus and stratocumulus clouds (Eastman et al., 2011, Lebsack
251 et al., 2011, Wood 2012, Zhou et al., 2015). Sea salt dry deposition (turbulent) and
252 sedimentation also contribute to its removal from low altitudes. Interestingly, the
253 sedimentation process plays the smallest removal role for the sea salt particles with
254 diameter less than 3 μm , whereas it overwhelmingly controls sea salt loss rate (i.e. more
255 than 1.5 times those of all other processes combined) when coarser mode sea salt is
256 included (see Table 1 column 3). This is expected because nearly 90% of injected sea salt
257 mass is in coarse mode based on our emission scheme. Since sea salt is found mostly in

258 the lower atmosphere, further removal of sea salt particles by cold clouds was found to
259 have only marginal impact on its mass budget in our sensitivity studies, although its
260 feedback on cold clouds needs further study. Note that results in Table 1 are summarized
261 on an annual basis from July 2016 to June 2017.

262

263 Atmospheric convection impacts the sea salt vertical distribution as well. The height of
264 the turnaround level (or the transition layer) between two vertical distribution regimes in
265 Fig. 3 is around 600 hPa in the polar regions and moves up to 400 hPa in the tropical
266 region, given that more vigorous convective activities occur in the tropical region. The
267 seasonal variation of the vertical gradient is larger in polar regions than in tropical region,
268 consistent with stronger seasonal variations of the meteorological fields (e.g. T, RH,
269 wind, etc) in high latitudes.

270

271 **4.3 Marine aerosol AOD**

272 To provide an overall picture of sea salt for this study, we compared the GEOS AOD
273 with satellite MODIS Collection 6 (C6) Aerosol AOD retrieval (Levy et al., 2013) and
274 AERONET Maritime Aerosol Network (MAN) measurements (Smirnov et al., 2017)
275 focusing on sea salt dominated regions. AOD integrates extinction by all aerosols in the
276 atmospheric column, with extinction dependent on the absolute mass, size distribution,
277 hygroscopic growth, vertical distribution, and optical property of each individual
278 component and the composition of aerosols.

279

280 Figure 4 shows total AOD comparison between MODIS and GEOS in August 2016 and
281 February 2017. Here, the GEOS AODs are sampled using daily MODIS AOD retrieval.
282 The AODs are only shown where the fraction of sea salt AOD relative to the total aerosol
283 AOD simulated by GEOS (fSSAOD, bottom panel) is larger than 0.6 so that we can
284 focus our discussion over sea salt dominant regions. MODIS AODs are much higher than
285 GEOS AODs for both seasons over remote oceans where sea salt dominates, by 0.043 in
286 August 2016 and 0.062 in February 2017. These differences between MODIS and GEOS
287 are higher than the potential positive bias of MODIS C6 AOD, up to 0.03, over oceans
288 (Figure 16 in Levy et al., 2013). It is difficult for us to remove the MODIS bias in the
289 comparison shown in the Figure 4 since the study of Levy et al., (2013) gave only
290 statistic value of MODIS AOD bias without the information of geophysical location.

291
292 The conclusion of a lower GEOS AOD can also be found in Fig. 5 by comparing AOD
293 between ground-based shipboard measurements and the GEOS simulations. AERONET
294 MAN provides ship-borne aerosol optical depth measurements from Microtops II sun
295 photometers. The MAN data is not found to have the positive systematic bias reported for
296 MODIS. MAN measurements from July, 2016 to June 2017 are used in this study. The
297 GEOS model results are sampled at the closest time and location of the ship-based
298 measurements. The model AODs are much smaller than MAN measurements over a
299 majority of the open ocean areas except part of the Atlantic Ocean where AOD was
300 impacted by dust. The scatter plot at the bottom of the figure indicates clearly that the
301 modeled AOD is biased low, especially over the Southern Ocean where the model AOD
302 is less than half of MAN's.

303

304 On the one hand, GEOS's sea salt mass is comparable to SAGA *in situ* measurements in
305 the MBL, and on the other hand, GEOS underestimates AOD when compared with
306 measurements from MAN and MODIS. The agreement with PALMS vertical gradients
307 shows that the AOD cannot be explained by sea salt above the MBL. There are various
308 potential reasons for this conundrum, such as the sea salt size distribution, atmospheric
309 relative humidity, sea salt particle hygroscopic growth rate, sea salt refractive index, etc.
310 We will discuss the first two potential reasons below.

311

312 **4.4 Size distribution and atmospheric RH**

313 The sea salt size distribution is a key factor in AOD calculation because small particles
314 are more optically efficient [at light extinction](#). [Aerosol size](#) also [modulates the](#) transport
315 and removal processes. The necessity to study sea salt size distribution lies also in [the](#)
316 important role [of sea salt particle sizes that affects](#) atmospheric chemistry, radiative
317 effects, and cloud formation processes.

318

319 To [compare the sea salt size distributions between the model and ATom data](#), we
320 calculate normalized percentage of sea salt mass in each of the first three size bins for
321 PALMS and GEOS over three atmospheric vertical layers for ATom1 and 2, as shown in
322 Figure 6. The three vertical layers (i.e. 0-1.5, 1.5-6, and >6 km) represent the boundary
323 layer, middle troposphere, and upper troposphere. GEOS sea salt particle mass and size
324 have been computed at RH of 45% to match the measurement condition of PALMS. [The](#)
325 particle sizes [here](#) are limited to be less than 3 μm in dry diameter due to [the size cut of](#)

326 the PALMS inlet. Particles in this range are most important in light extinction and cloud
327 formation with many more sea salt particles in fine mode than in coarse mode on a per
328 unit mass basis.

329
330 Figure 6 reveals that the size distribution is more flat in PALMS than in GEOS. In other
331 words, with the same sea salt mass, the fraction of sea salt in the finest mode in PALMS
332 is much larger (i.e. about 5-7 times higher) than in GEOS. To quantify the potential
333 impact of sea salt size distribution on AOD calculation, we calculate the sea salt mass
334 extinction efficiency (MEE) integrated over the three bins using the two size distributions
335 of PALMS and GEOS at RH 45% and 550 nm in the same three vertical layers and in the
336 whole atmosphere (Table 2). The size segregated MEEs used in the calculation are 1.6,
337 5.6, and 1.2 m² g⁻¹ for the bins 1-3, respectively. The effective MEE from GEOS for the
338 size range is 1.7 m² g⁻¹, which is about 24% lower than 2.2 m² g⁻¹ calculated with the
339 PALMS size distribution. Thus, the underestimation of GEOS AOD shown in Figure 5c
340 may partially stem from the model underestimate of the small sea salt particles, especially
341 for those with diameter less than 1 μm (Figure 6). The underestimation of AOD by GEOS
342 is more significant in the boundary layer shown in Table 2, which implies that the sea salt
343 size distribution from emission may need to be revisited.

344
345 Apparently, sea salt size distribution is a potential culprit for the dichotomy in GEOS
346 simulation since GEOS partitions more sea salt onto larger particles that are less optically
347 active compared with the significant fine sea salt mode observed in PALMS
348 measurements. Such large underestimation of fine sea salt particles by the model may

349 have significant implications not only on the AOD calculation but also on studies of
350 radiative effects and cloud formation because particle number concentration is a key
351 quantity for these processes. The conclusion that GEOS sea salt size distribution favors
352 the coarse mode sea salt particles is consistent with a recent study of Naumann et al.,
353 (2016), which found that the sea salt emission of Gong (2003) yielded overestimations in
354 the PM10 measured at coastal stations and underestimations at inland stations over
355 northwestern Europe.

356

357 Sea salt particle size distribution changes horizontally and vertically, but the change is
358 much smaller than the difference between those of model and measurement. This implies
359 a possibility of using a global size distribution without sacrificing much accuracy.

360

361 Another possible contribution to underestimation of the AOD due to sea salt in the model
362 is if there is a general underestimate in the humidification of sea salt particles in the
363 model, with a corresponding underestimate on optical efficiency per unit dry mass.

364 Figure 7 compares atmospheric RHs between ATom measurements and GEOS
365 simulations along flight tracks summarized over the same regions as in Fig. 3. With only
366 a few exceptions, the model RH is higher than the ATom measurements, including in the
367 MBL_s where humidity is typically high. Thus, atmospheric water vapor simulation is not
368 responsible for the low AOD calculation. In fact, using measured RH along with the
369 model's sea salt size distribution and vertical distribution would give even lower AOD.
370 There should be other factors contributing to a lower GEOS AOD calculation as well,
371 such as sea salt hygroscopic growth rate, sea salt optical properties, and other aerosol

372 species over ocean. Further investigations for these factors are needed to better
373 understand the GEOS sea salt simulation.

374

375 **Conclusions**

376 A systematic and comprehensive global sea salt study was conducted by integrating
377 NASA GEOS model simulations with ATom *in situ* measurements from the PALMS and
378 SAGA instruments, as well as AOD measurements from AERONET MAN and satellite
379 MODIS over the oceans. This work takes advantage of PALMS sea salt vertical profile
380 measurement together with SAGA filter measurements in MBL, covering global remote
381 regions over the Pacific, Atlantic, and Southern Oceans from near the surface to ~12 km
382 altitude and *in* both summer and winter seasons. Important atmospheric sea salt fields,
383 e.g. mass mixing ratio, vertical distribution, size distribution, and aerosol AOD, are
384 examined. The meteorological field of RH and the sea salt simulation processes of
385 emission, dry deposition, sedimentation, and large scale and convective wet depositions
386 were explored to explain the sea salt fields and to reveal a potential direction for model
387 improvement.

388

389 Generally, the agreement between ATom measurements and the model is remarkable,
390 both in terms of absolute loading and especially in the shape of the vertical distribution
391 under a *wide range* of *different* tropospheric environments. The correlation coefficients
392 are generally higher than 0.8 between GEOS-PALMS and GEOS-SAGA for both ATom1
393 and ATom2 periods. GEOS results capture the strong sea salt vertical gradient shown in
394 the measurements except over SH high latitudes, where the PALMS's gradient is deeper.

395 In the MBL, the current GEOS sea salt simulation is comparable (ATom1) or slightly
396 higher (ATom2) than SAGA data, which in turn is higher than PALMS data.

397

398 An underestimation of GEOS aerosol AOD over sea salt dominated oceans is found from
399 the comparison of AODs between GEOS and MAN, as well as GEOS and MODIS. This
400 is contradictory to the finding that GEOS sea salt mass abundance is comparable to or
401 slightly higher than measurements. This conundrum may be partially attributed to the
402 difference in sea salt mass size distributions between GEOS and PALMS. The GEOS sea
403 salt mass size distribution favors the coarse mode while PALMS has a larger fraction of
404 more optically active submicron sea salt. The atmospheric water vapor, however, can be
405 ruled out as the cause of model underestimation of AOD, since the GEOS RH is
406 comparable to or higher than ATom measurements almost everywhere along the flight
407 tracks, especially in MBL.

408

409 Atmospheric sea salt vertical distribution is impacted by various processes including
410 emission, hygroscopic growth, dry deposition, sedimentation, wet deposition, convection,
411 and large-scale advection. Among these processes, wet deposition, owing to both shallow
412 marine cloud structure and rapid hygroscopic growth of sea salt particles, is most
413 important in shaping the vertical profile for the size range studied in this work and results
414 in a sharp gradient in the low atmosphere where RH is typically very high. Vertical
415 convection is also important for explaining the sea salt vertical profiles.

416

417 More work is needed in the future to investigate sea salt hygroscopic growth rate, optical
418 properties, sea water salinity, sea ice, and marine organic aerosol to understand the
419 dilemma in GEOS simulation. Consideration of variations in salinity of surface seawater is
420 missing in the GEOS aerosol model. Although salinity may not be an important factor in
421 sea salt emission on the global scale owing to its relatively uniformity across the world
422 oceans, it may be important regionally as discussed by Grythe et al., (2014). Salinity also
423 impacts sea spray aerosol (SSA) size. The dry SSA size distribution shifts towards
424 smaller sizes with lower salinities found in the EMEP intensive campaigns (Barthel et al.,
425 2014). Sea ice, whose contribution is also neglected in the GEOS aerosol model, could be
426 an important source of sea salt aerosol over polar regions and has significant implications
427 for polar climate and atmospheric chemistry reported by recent publications (Dall et al.,
428 2017; May et al., 2016; Rhodes et al., 2017). More importantly, primary marine organic
429 aerosols (Randles et al., 2004), which come also from sea spray bubble bursting as sea
430 salts but are more submicron particles, should be investigated to disentangle the sea spray
431 aerosols.

432

433 **Author contribution**

434 Huisheng Bian and Mian Chin designed the experiments. Peter R. Colarco, Anton Darmanov,
435 Arlindo da Silva, Tom L. Kucsera, and Hongbin Yu contributed to GEOS-GOCART model setup
436 and provided tools to analyze model data. Huisheng Bian conducted the model simulation and in
437 charge of the analyses. Karl Froyd, Daniel M. Murphy, and Gregory Schill provided ATom
438 PALMS measurement data. Jack Dibb provided ATom SAGA measurement data. Maximilian
439 Dollner and Bernadett Weinzierl provided ATom CAPS cloud data. Paul Bui provided ATom
440 MMS data for RH measurement. Hongbin Yu and Alexander Smirnov provided MODIS satellite

441 and AERONET MAN measurement data. All authors contributed to the data analyses and paper
442 writing.

443

444

445 **Acknowledgments**

446

447 This research was supported by two programs of the National Aeronautics and Space
448 Administration (NASA): Atmospheric Composition: Modeling and Analysis Program
449 (ACMAP) and Earth Venture-suborbital program for the Atmospheric Tomography
450 Mission (ATom).

451

452 **References:**

453

454 Alexander, B., R. J. Park, D. J. Jacob, Q. B. Li, R. M. Yantosca, J. Savarino, C. C. W. Lee, and
455 M. H. Thiemens (2005), Sulfate formation in sea-salt aerosols: Constraints from oxygen i
456 sotopes, *J. Geophys. Res.*, 110, D10307, doi:10.1029/2004JD005659.

457 Anastasio, C. and Newberg, J. T.: Sources and sinks of hydroxyl radical in sea-salt particles, *J.*
458 *Geophys. Res.*, 112, D10306, doi:10.1029/2006JD008061, 2007.

459 Barthel, S., Tegen, I., Wolke, R., and van Pinxteren, M.: Model study on the dependence of
460 primary marine aerosol emission on the sea surface temperature, *Atmos. Chem. Phys. Discuss.*,
461 14, 377-434, <https://doi.org/10.5194/acpd-14-377-2014>, 2014.

462 Bian, H., Chin, M., Hauglustaine, D. A., Schulz, M., Myhre, G., Bauer, S. E., Lund, M. T.,
463 Karydis, V. A., Kucsera, T. L., Pan, X., Pozzer, A., Skeie, R. B., Steenrod, S. D., Sudo, K.,
464 Tsigaridis, K., Tsimpidi, A. P., and Tsyro, S. G.: Investigation of global nitrate from the

465 AeroCom Phase III experiment, *Atmos. Chem. Phys.*, 17, 12911-12940,
466 <https://doi.org/10.5194/acp-17-12911-2017>, 2017.

467 Bian, H., P. Colarco, M. Chin, G. Chen, J.M. Rodriguez, Q. Liang, et al., Investigation of source
468 attributions of pollution to the Western Arctic during the NASA ARCTAS field campaign.
469 *Atmos. Chem. and Phys.*, 13, 4707-4721, doi:10.5194/acp-13-4707-2013, 2013.

470 Browse, J., Carslaw, K. S., Mann, G. W., Birch, C. E., Arnold, S. R., and Leck, C.: The complex
471 response of Arctic aerosol to sea-ice retreat, *Atmos. Chem. Phys.*, 14, 7543-7557,
472 <https://doi.org/10.5194/acp-14-7543-2014>, 2014.

473 Chin, M., T. Diehl, Q. Tian, J. M. Prospero, R. A. Kahn, A. Remer, H. Yu, A. M. Sayer, H. Bian,
474 et al., Multi-decadal variations of atmospheric aerosols from 1980 to 2009: sources and regional
475 trends, *Atmos. Chem. Phys.*, 14, 3657-3690, doi:10.5194/acp-14-3657-2014, 2014.

476 Chin, M., P. Ginoux, S. Kinne, B. N. Holben, B. N. Duncan, R. V. Martin, J. A. Logan, A.
477 Higurashi, and T. Nakajima, 2002: Tropospheric aerosol optical thickness from the GOCART
478 model and comparisons with satellite and sun photometer measurements, *J. Atmos. Sci.* 59, 461-
479 483.

480 Colarco, P., da Silva, A., Chin, M., and Diehl, T.: On-line simulations of global aerosol
481 distributions in the NASA GEOS-4 model and comparisons to satellite and ground based aerosol
482 optical depth, *J. Geophys. Res.*, 115, D14207, doi:10.1029/2009JD012820, 2010.

483 Dadashazar, H., Wang, Z., Crosbie, E., Brunke, M., Zeng, X., Jonsson, H., Woods, R. K., Flagan,
484 R. C., Seinfeld, J. H., and Sorooshian, A.: Relationships between giant sea salt particles and
485 clouds inferred from aircraft physico-chemical data, *J. Geophys. Res.-Atmos.*, 122, 3421-3434,
486 <https://doi.org/10.1002/2016JD026019>, 2017.

487 *Dall'Osto, M., Geels, C., Beddows, D.C.S., Boertmann, D., Lange, R., Nøjgaard, J.K., Harrison*
488 *Roy, M., Simo, R., Skov, H., Massling, A., 2018. Regions of open water and melting sea ice drive*
489 *new particle formation in North East Greenland. Sci. Rep. 8,6109.*

490 *Dall'Osto, M., Beddows, D.C.S., Tunved, P., Krejci, R., Ström, J., Hansson, H.-C., Yoon, Y.J.,*
491 *Park, Ki-Tae, Becagli, S., Udisti, R., Onasch, T., O'Dowd, C.D., Simó, R., Harrison, Roy M.,*
492 *2017a. Arctic sea ice melt leads to atmospheric new particle formation. 2017. Scientific Reports*
493 *7, P. 3318. <https://doi.org/10.1038/s41598-017-03328-1>.*
494 *Darmenov, A., da Silva, A., Liu, X. and Colarco, P. R., (2013), Data-driven aerosol development*
495 *in the GEOS-5 modeling and data assimilation system, Abstract A43D-0305 presented at 2013*
496 *Fall Meeting, AGU, San Francisco, Calif, 9-13 Dec.*
497 *de Leeuw, G., Andreas, E. L., Anguelova, M. D., Fairall, C.W., Lewis, E. R., O'Dowd, C., Schulz,*
498 *M., and Schwartz, S. E.: Production flux of sea spray aerosol, Rev Geophys, 49, RG2001,*
499 *doi:10.1029/2010rg000349, 2011.*
500 Eastman, R., S. G. Warren, and C. J. Hahn, 2011: Variations in cloud cover and cloud types over
501 the ocean from surface observations, 1954–2008. *J. Climate*, 24, 5914–5934.
502 *Froyd, K. D., Murphy, D. M., Brock, C. A., Campuzano-Jost, P., Dibb, J. E., Jimenez, J.-L., Kupc,*
503 *A., Middlebrook, A. M., Schill, G. P., Thornhill, K. L., Williamson, C. J., Wilson, J. C., and*
504 *Ziembra, L. D.: A new method to quantify mineral dust and other aerosol species from aircraft*
505 *platforms using single particle mass spectrometry, Atmos. Meas. Tech. Discuss.,*
506 *<https://doi.org/10.5194/amt-2019-165>, in review, 2019.*
507 Gelaro, R., McCarty, W., Suárez, M. J., Todling, R., Molod, A., Takacs, L., Randles, C. A.,
508 Darmenov, A., Bosilovich, M. G., Reichle, R., Wargan, K., Coy, L., Cullather, R., Draper, C.,
509 Akella, S., Buchard, V., Conaty, A., da Silva, A. M., Gu, W., Kim, G. K., Koster, R., Lucchesi,
510 R., Merkova, D., Nielsen, J. E., Partyka, G., Pawson, S., Putman, W., Rienecker, M., Schubert, S.
511 D., Sienkiewicz, M., and Zhao, B.: The Modern-Era Retrospective Analysis for Research and
512 Applications, Version 2 (MERRA-2), *J. Climate*, 30, 5419–5454, [https://doi.org/10.1175/JCLI-D-](https://doi.org/10.1175/JCLI-D-16-0758.1)
513 [16-0758.1](https://doi.org/10.1175/JCLI-D-16-0758.1), 2017.
514 Gerber, H. E. (1985), Relative-humidity parameterization of the Navy aerosol model (NAM),
515 NRL Rep. 8956, Naval Res. Lab., Washington, D. C.

516 *Grini, A., M. Myhre, J. K. Sundet, and I. S. A. Isaksen, Modeling the Annual Cycle of Sea Salt in*
517 *the Global 3D Model Oslo CTM2: Concentrations, Fluxes, and Radiative Impact, Journal of*
518 *Climate, 15(13), 1717–1730. [https://doi.org/10.1175/1520-0442\(2002\)](https://doi.org/10.1175/1520-0442(2002)).*

519 Gong, S. L., A parameterization of sea-salt aerosol source function for sub- and super-micron
520 particles, *Global Biogeochem. Cycles*, 17 (4), 1097, doi:10.1029/2003GB002079, 2003.

521 *Grythe, H., Ström, J., Krejci, R., Quinn, P., and Stohl, A.: A review of sea-spray aerosol source*
522 *functions using a large global set of sea salt aerosol concentration measurements, Atmos. Chem.*
523 *Phys., 14, 1277-1297, <https://doi.org/10.5194/acp-14-1277-2014>, 2014.*

524 Intergovernmental Panel on Climate Change (IPCC) 2001 In *Climate Change 2001: The*
525 *Scientific Basis* (eds J. T. Houghton, Y. Ding, D. J. Griggs, M. Noguer, P. J. van der Linden and
526 D. Xiaosu), New York, NY: Cambridge University Press.

527 Jacobson, M. Z. (2001), Global direct radiative forcing due to multicomponent anthropogenic and
528 natural aerosols, *J. Geophys. Res.*, 106(D2), 1551-1568.

529 Jaeglé, L., Quinn, P. K., Bates, T. S., Alexander, B., and Lin, J.-T.: Global distribution of sea salt
530 aerosols: new constraints from insitu and remote sensing observations, *Atmos. Chem. Phys.*, 11,
531 3137–3157, doi:10.5194/acp-11-3137-2011, 2011.

532 Kogan, Yefim L., David B. Mechem, Kityan Choi, Effects of Sea-Salt Aerosols on Precipitation
533 in Simulations of Shallow Cumulus, <https://doi.org/10.1175/JAS-D-11-031.1>, 2012.

534 Keene W. C., Psexenny A. A. P., Galloway J. N. and Hawley M. E. (1986) Seasalt corrections and
535 interpretation of constituent ratios in marine precipitation. *J. Geophys. RES.* 91,6647-6658.

536 Kishcha, P., Nickovic, S., Starobinetes, B., di Sarra, A., Udisti, R., Becagli, S., Sferlazzo, D.,
537 Bommarito, C., Alpert, P., 2011. Sea-salt aerosol forecasts compared with daily measurements at
538 the island of Lampedusa (Central Mediterranean). *Atmospheric Research* 100, 28-35.

539 Lawler, M. J., Sander, R., Carpenter, L. J., Lee, J. D., von Glasow, R., Sommariva, R., and
540 Saltzman, E. S.: HOCl and Cl₂ observations in marine air, *Atmos. Chem. Phys.*, 11, 7617-7628,
541 <https://doi.org/10.5194/acp-11-7617-2011>, 2011.

542 Lebock MD, L'Ecuyer TS, Stephens GL (2011) Detecting the ratio of rain and cloud water in
543 low-latitude shallow marine clouds. *J Appl Meteorol Climatol* 50:419-432.
544 <https://doi.org/10.1175/2010JAMC2494.1>.

545 Levy, R. C., Mattoo, S., Munchak, L. A., Remer, L. A., Sayer, A. M., Patadia, F., and Hsu, N. C.:
546 The Collection 6 MODIS aerosol products over land and ocean, *Atmos. Meas. Tech.*, 6, 2989-
547 3034, <https://doi.org/10.5194/amt-6-2989-2013>, 2013.

548 Lewis, E.R., Schwartz, S.E., 2004. Sea salt aerosol production: mechanisms, methods,
549 measurements and models - a critical review. *Geophysical Monograph*, vol. 152. Print
550 ISBN:9780875904177 |Online ISBN:9781118666050 |DOI:10.1029/GM152, American
551 Geophysical Union, Washington, DC.

552 May, N. W., Quinn, P. K., McNamara, S. M., and Pratt, K. A.: Multiyear study of the dependence
553 of sea salt aerosol on wind speed and sea ice conditions in the coastal Arctic, *J. Geophys. Res.*-
554 *Atmos.*, 121, 9208–9219, <https://doi.org/10.1002/2016JD025273>, 2016.

555 McNaughton, C. S., Clarke, A. D., Howell, S. G., Pinkerton, M., Anderson, B., Thornhill, L.,
556 Hudgins, C., Winstead, E., Dibb, J. E., Scheuer, E., and Maring, H.: Results from the DC-8 Inlet
557 Characterization Experiment (DICE): Airborne Versus Surface Sampling of Mineral Dust and
558 Sea Salt Aerosols, *Aerosol. Sci. Tech.*, 41, 136–159, 2007.

559 *Murphy, D. M., Froyd, K. D., Bian, H., Brock, C. A., Dibb, J. E., DiGangi, J. P., Diskin, G.,*
560 *Dollner, M., Kupc, A., Scheuer, E. M., Schill, G. P., Weinzierl, B., Williamson, C. J., and Yu, P.:*
561 *The distribution of sea-salt aerosol in the global troposphere, Atmos. Chem. Phys.*, 19, 4093-
562 4104, <https://doi.org/10.5194/acp-19-4093-2019>, 2019.

563 Neumann, D., Matthias, V., Bieser, J., Aulinger, A., and Quante, M.: A comparison of sea salt
564 emission parameterizations in north-western Europe using a chemistry transport model setup,
565 *Atmos. Chem. Phys.*, 16, 9905–9933, doi:10.5194/acp-16-9905-2016, 2016.

566 Pierce, J. R., and P. J. Adams (2006), Global evaluation of CCN formation by direct emission of
567 sea salt and growth of ultrafine sea salt, *J. Geophys. Res.*, 111, D06203,
568 doi:10.1029/2005JD006186.

569 [Quinn](#) PK and TS Bates, *Ocean-Derived Aerosol and Its Climate Impacts*, 5.12, Published by
570 Elsevier Ltd., 2013.

571 *Prospero, J. M., Savoie, D. L., and Arimoto, R.: Long-term record of nss-sulfate and nitrate in*
572 *aerosols on Midway Island, 1981–2000: evidence of increased (now decreasing?) anthropogenic*
573 *emissions from Asia, J. Geophys. Res., 108, 4019, doi:10.1029/2001JD001524, 2003.*

574
575 Randles, C. A., Russell, L. M., and Ramaswamy, V.: Hygroscopic and optical properties of
576 organic sea salt aerosol and consequences for climate forcing, *Geophys. Res. Lett.*, 31, L16 108,
577 doi:10.1029/2004GL020628, 2004.

578 Randles, C. A., da Silva, A. M., Buchard, V., Colarco, P. R., Darmenov, A., Govindaraju, R.,
579 Smirnov, A., Holben, B., Ferrare, R., Hair, J., Shinozuka, Y., and Flynn, C. J.: The MERRA-2
580 Aerosol Reanalysis, 1980-onward, Part I: System Description and Data Assimilation Evaluation,
581 *J. Climate*, 30, 6823–6850, <https://doi.org/10.1175/jcli-d-16-0609.1>, 2017.

582 Rhodes, R. H., Yang, X., Wolff, E. W., McConnell, J. R., and Frey, M. M.: Sea ice as a source of
583 sea salt aerosol to Greenland ice cores: a model-based study, *Atmos. Chem. Phys.*, 17, 9417–
584 9433, <https://doi.org/10.5194/acp-17-9417-2017>, 2017.

585 Rienecker, M. M., Suarez, M. J., Gelaro, R., Todling, R., Bacmeister, J., Liu, E., Bosilovich, M.
586 G., Schubert, S. D., Takacs, L., Kim, G. K., Bloom, S., Chen, J., Collins, D., Conaty, A., da Silva,
587 A., Gu, W., Joiner, J., Koster, R. D., Lucchesi, Andrea Molod, A., Owens, T., Pawson, S.,
588 Pegion, P., Redder, C. R., Reichle, R., Robertson, F. R., Ruddick, A. G., Sienkiewicz, M., and
589 Woollen, J.: MERRA: NASA’s Modern-Era Retrospective Analysis for Research and
590 Applications, *J. Climate*, 24, 3624–3648, 2011.

Formatted: Don't adjust space between Latin and Asian text, Don't adjust space between Asian text and numbers

591 Smirnov, A., M. Petrenko, C. Ichoku, and B. Holben. 2017. "Maritime Aerosol Network optical
592 depth measurements and comparison with satellite retrievals from various different sensors."
593 Remote Sensing of Clouds and the Atmosphere XXII, [10.1117/12.2277113].

594 Spada, M., Jorba, O., Pérez García-Pando, C., Janjic, Z., and Baldasano, J. M.: Modeling and
595 evaluation of the global sea-salt aerosol distribution: sensitivity to size-resolved and sea-surface
596 temperature dependent emission schemes, *Atmos. Chem. Phys.*, 13, 11735-11755,
597 <https://doi.org/10.5194/acp-13-11735-2013>, 2013.

598 Spada, M., Jorba, O., Pérez García-Pando, C., Janjic, Z., and Baldasano, J. M.: On the evaluation
599 of global sea-salt aerosol models at coastal/orographic sites, *Atmos. Environ.*, 101, 41–48,
600 <https://doi.org/10.1016/j.atmosenv.2014.11.019>, 2015

601 Takemura, T., Nakajima, T., Dubovik, O., Holben, B. N., and Kinne, S.: Single-scattering albedo
602 and radiative forcing of various aerosol species with a global three-dimensional model, *J.*
603 *Climate*, 15(4), 333–352, 2002

604 Textor, C., Schulz, M., Guibert, S., Kinne, S., Balkanski, Y., Bauer, S., Bernsten, T., Berglen, T.,
605 Boucher, O., Chin, M., Dentener, F., Diehl, T., Easter, R., Feichter, H., Fillmore, D., Ghan, S.,
606 Ginoux, P., Gong, S., Grini, A., Hendricks, J., Horowitz, L., Huang, P., Isaksen, I., Iversen, I.,
607 Kloster, S., Koch, D., Kirkevåg, A., Kristjansson, J. E., Krol, M., Lauer, A., Lamarque, J. F., Liu,
608 X., Montanaro, V., Myhre, G., Penner, J., Pitari, G., Reddy, S., Seland, Ø., Stier, P., Takemura,
609 T., and Tie, X.: Analysis and quantification of the diversities of aerosol life cycles within
610 AeroCom, *Atmos. Chem. Phys.*, 6, 1777–1813, <https://doi.org/10.5194/acp-6-1777-2006>, 2006.

611 Tsyro, S., W. Aas, J. Soares, M. Sofiev, H. Berge, and G. Spindler, Modelling of sea salt
612 concentrations over Europe: key uncertainties and comparison with observations, *Atmos. Chem.*
613 *Phys.*, 11, 10367–10388, 2011, www.atmos-chem-phys.net/11/10367/2011/, doi:10.5194/acp-11-
614 10367-2011.

615 Wilson, T. R. S., Salinity and the major elements of sea water, in *Chemical Oceanography*, vol. 1,
616 2nd ed., edited by J.P. Riley and G. Skirrow, pp. 365-413, Academic, Orlando, Fla., 1975.

617 Witek, M. L., P. J. Flatau, P. K. Quinn, and D. L. Westphal, 2007: Global sea-salt modeling:
618 Results and validation against multicampaign shipboard measurements. *J. Geophys. Res.*, 112,
619 D08215, doi:10.1029/2006JD007779.
620 Wood, R., 2012. Stratocumulus clouds. *Month. Weath. Rev.* 140, 2373–2423.
621 Zhou, X., Kollias, P., & Lewis, E. R. (2015). Clouds, precipitation, and marine boundary layer
622 structure during the MAGIC field campaign. *Journal of Climate*, 28(6), 2420–2442.
623 <https://doi.org/10.1175/JCLI-D-14-00320.1>.

625
626
627
628
629

Table 1. Sea salt (SS) budget analysis on annual basis from July 2016 to June 2017 (the 2th column: GEOS SS up to 3 μm in dry diameters, the 3th column: GEOS SS for all bins, and the 4th column AeroCom SS for all bins).

	GEOS SS (Dp ^a < 3μm)	GEOS SS (all bins)	AeroCom SS (all bins)
Emission (Tg/yr)	515.2	4015.5	2190-117949
Burden (Tg)	1.63	6.80	3.4-18.2
Lifetime (days)	1.16	0.62	0.03-1.59
Surf concentration (μg/kg)	3.2	16.5	
Dry deposition (Tg/yr)	103.1	460.9	
Sedimentation (Tg/yr)	61.1	2458.2	
Kdry ^b (days ⁻¹)	1.17	1.17	0.06-2.94
LS ^c deposition (Tg/yr)	140.3	354.7	
SV ^d deposition (Tg/yr)	211.8	746.1	
Kwet ^e (days ⁻¹)	0.44	0.44	0.11-2.45
SSAOD _{550nm}		0.0269	0.003-0.067

630 ^aDp: particle diameter (μm)
631 ^bKdry: loss frequency due to dry deposition and sedimentation (days⁻¹)
632 ^cLS: large scale wet deposition (Tg/yr)
633 ^dSV: convective wet deposition (Tg/yr)
634 ^eKwet: loss frequency due to wet large scale and convective depositions (days⁻¹)

635
636
637
638
639
640

Table 2. Sea salt mass extinction efficient (MEE) for PALMS and GEOS and the ratio of MEEs between GEOS and PALMS in three vertical layers and in the whole atmosphere at RH 45%

	PALMS (m ² /kg)	GEOS (m ² /kg)	R(GEOS/PALMS) %
0 – 1.5 KM	2636.87	1618.09	61.4
1.5 – 6 KM	2089.97	1671.61	80.0
>6 KM	1891.07	1786.24	94.5
all	2203.67	1679.36	76.2

641

642

643 **Figure Captions**

644 **Figure 1.** AToM1 (top) and AToM2 (bottom) flight track sorted out for each flight day.

645

646 **Figure 2a.** Scatter plot of sea salt between GEOS and PALMS (magenta) and between

647 GEOS and SAGA (blue) in AToM1 (symbol +) and AToM2 (symbol \diamond) for all flight

648 measurements within 1.5 km atmospheric thickness above ocean surface. The SAGA

649 samples are filtered out when dust signal is significant. The GEOS sea salt shown here

650 are cut at 3 μm in dry diameters. Both GEOS and PALMS data are then sampled using

651 SAGA measurement time frequency. The statistical parameter r is the correlation

652 coefficient and b is the ratio of SS(GEOS) to SS(ATom).

653

654 **Figure 2b.** Similar to Figure 2a with the samples contaminated by clouds are further

655 excluded using CAPS cloud indicator.

656

657 **Figure 3.** Sea salt ($D_p < 3 \mu\text{m}$) vertical profiles from GEOS simulation and PALMS

658 measurement along AToM1 and 2 flight tracks in 5 latitudinal bands over Pacific and

659 Atlantic oceans. The latitudinal bands are marked by dot grey lines in Figure 1.

660

661 **Figure 4.** Total aerosol AOD in 201608 (left column) and 201702 (right column) from

662 MODIS (top) and GEOS (middle). The bottom panel shows the mass fraction of sea salt

663 relative to the total aerosol simulated by GEOS.

664

665 **Figure 5.** Total AOD measured by MAN cruise occurred during 201607 to 201706 (5a)
666 and simulated by GEOS but sampled with MAN measurement (5b). 5c shows total AOD
667 scattering plot between MAN and GEOS and the purple color is for the data over
668 Southern Ocean shown inside the boxes in Figure 5b.

669

670 **Figure 6.** Percentage distribution of sea salt mass over the first three bins normalized to
671 the total sea salt with particle wet diameter up to $\sim 5 \mu\text{m}$ at RH 45%. The normalized SS
672 mass weighting distribution is sorted over three vertical layers and for ATom1 (top row)
673 and ATom2 (bottom row), respectively.

674

675 **Figure 7.** Atmospheric RH vertical profiles from GEOS simulation and ATom
676 measurement along ATom1 and 2 flight tracks in 5 latitudinal bands over Pacific and
677 Atlantic oceans.

678

679

680

681

682

683

684

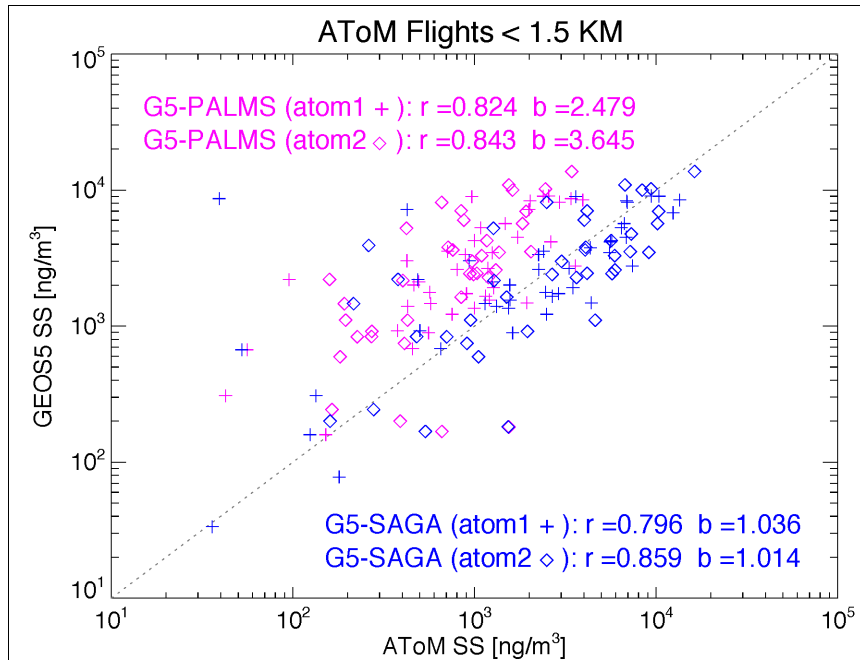


Figure 2a. Scatter plot of sea salt between GEOS and PALMS (magenta) and between GEOS and SAGA (blue) in AToM1 (symbol +) and AToM2 (symbol ◇) for all flight measurements within 1.5 km atmospheric thickness above ocean surface. The SAGA samples are filtered out when dust signal is significant. The GEOS sea salt shown here are cut at 3 μm in dry diameters. Both GEOS and PALMS data are then sampled using SAGA measurement time frequency. The statistical parameter r is the correlation coefficient and b is the ratio of $\text{SS}(\text{GEOS})$ to $\text{SS}(\text{AToM})$.

703
704
705
706

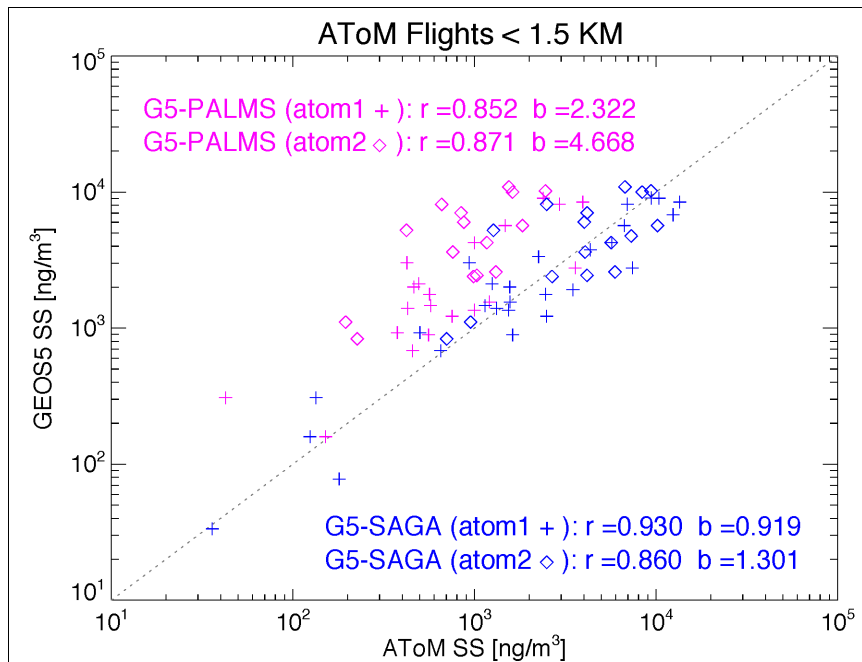


Figure 2b. Similar to Figure 2a with SAGA sodium data contaminated by clouds are further excluded using CAPS cloud indicator.

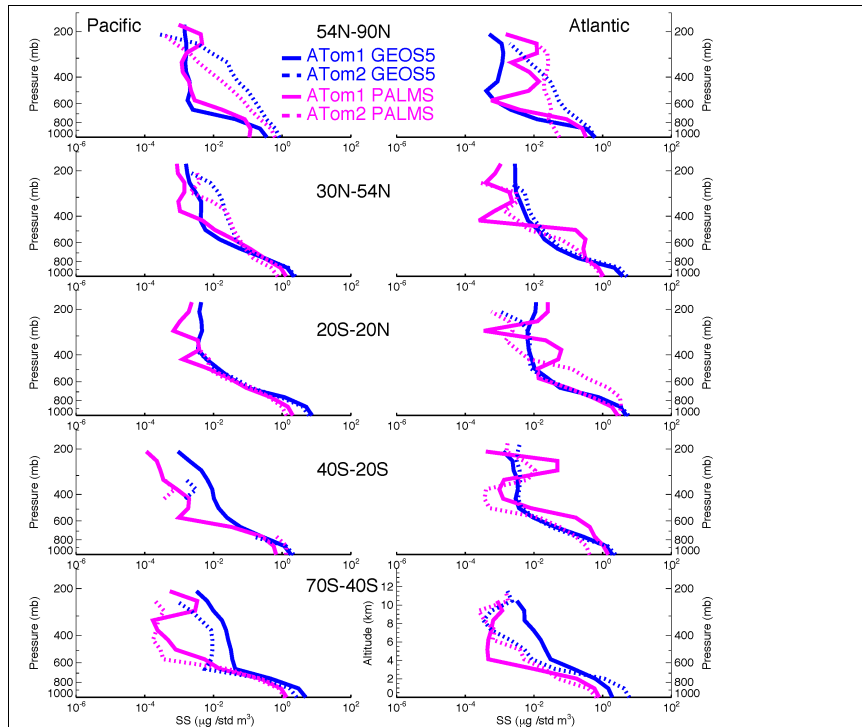


Figure 3. Sea salt ($D_p < 3 \mu\text{m}$) vertical profiles from GEOS5 simulation and PALMS measurement along ATom1 and 2 flight tracks in 5 latitudinal bands over Pacific and Atlantic oceans. The latitudinal bands are marked by dot grey lines in Figure 1.

707
 708
 709
 710
 711
 712
 713
 714
 715
 716
 717
 718
 719
 720
 721
 722

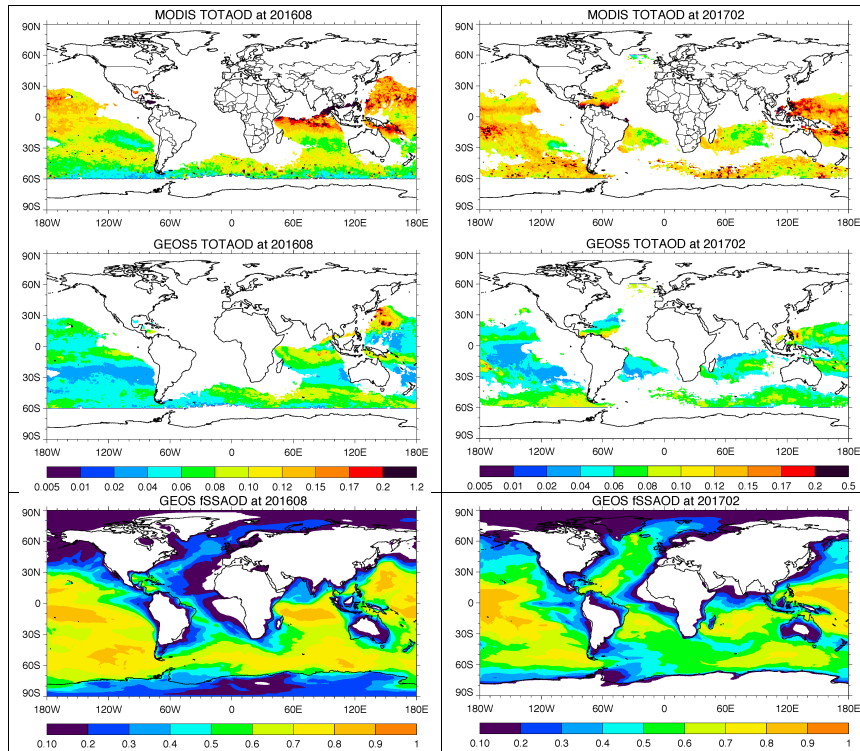


Figure 4. Total aerosol AOD in 201608 (left column) and 201702 (right column) from MODIS (top) and GEOS5 (middle) over oceans where fraction of sea salt AOD (fSSAOD) mass simulated by GEOS (bottom panel) is larger than 0.6.

723
 724
 725
 726
 727
 728
 729
 730
 731
 732
 733
 734
 735
 736
 737
 738

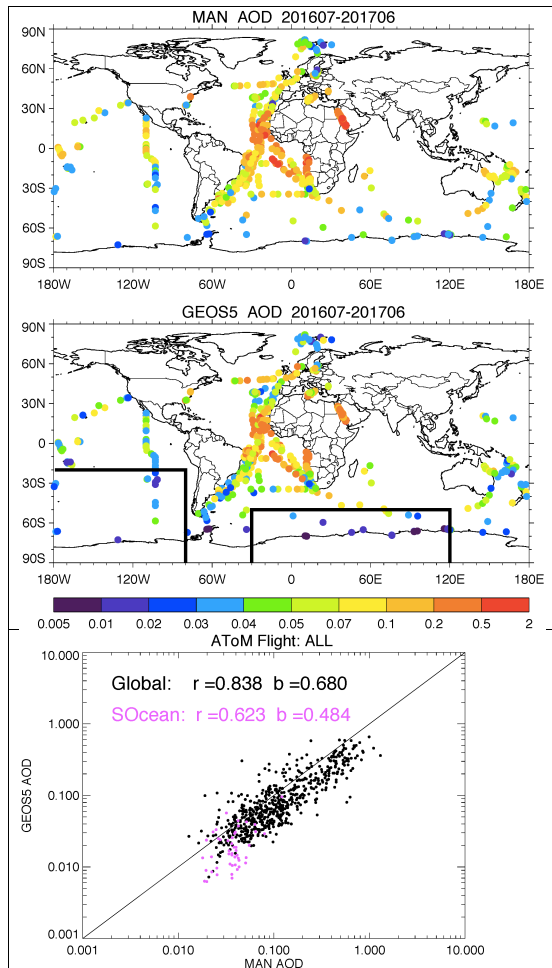


Figure 5. Total AOD measured by MAN cruise occurred during 201607 to 201706 (5a) and simulated by GEOS5 but sampled with MAN measurement (5b). 5c shows total AOD scattering plot between MAN and GEOS and the purple color is for the data over Southern Ocean shown inside the boxes in Figure 5b.

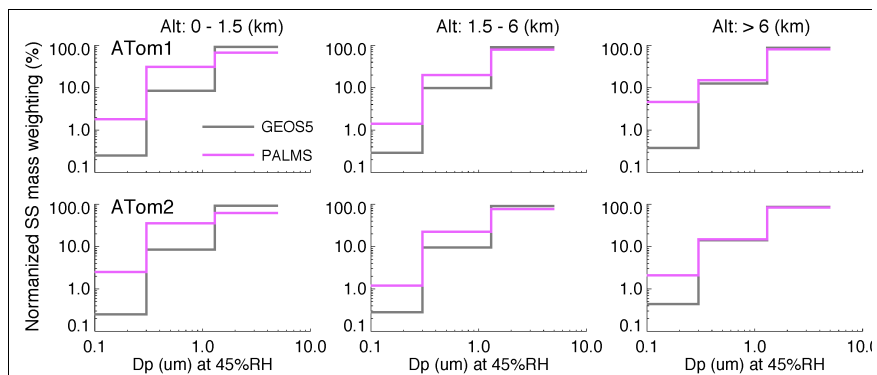


Figure 6. Percentage distribution of sea salt mass over the first three bins normalized to the total sea salt with particle wet diameter up to $\sim 5 \mu\text{m}$ at RH 45%. The normalized SS mass weighting distribution is sorted over three vertical layers and for ATom1 (top row) and ATom2 (bottom row), respectively.

744
745
746
747
748
749
750
751
752
753
754
755

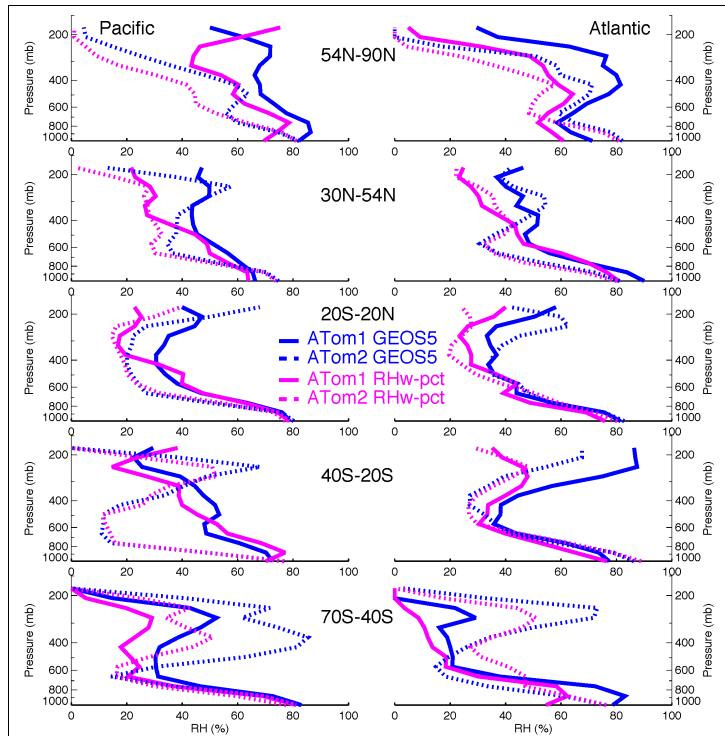


Figure 7. Atmospheric RH vertical profiles from GEOS5 simulation and ATom measurement along ATom1 and 2 flight tracks in 5 latitudinal bands over Pacific and Atlantic oceans.